Exploring nanopore direct sequencing performance of forensic STRs, SNPs, InDels, and DNA methylation markers in a single assay

de Bruin, Desiree D.S.H.; Haagmans, Martin A.; van der Gaag, Kristiaan J.; Hoogenboom, Jerry; Weiler, Natalie E.C.; Tesi, Niccoló; Holstege, Henne; Reinders, Marcel; Henneman, Peter; More Authors

Exploring nanopore direct sequencing performance of forensic STRs, SNPs, InDels, and DNA methylation markers in a single assay

Desiree D.S.H. de Bruin [a,b,1], Martin A. Haagmans [a,1], Kristiaan J. van der Gaag [c], Jerry Hoogenboom [c], Natalie E.C. Weiler [c], Niccoló Tesi [d,e], Alex Salazar [d], Yaran Zhang [d], Henne Holstege [d,e], Marcel Reinders [d,e], Amade Aouatef M'charek [f], Titia Sijen [c,g], Peter Henneman [a,h,i,*]

[a] Department of Human Genetics, Amsterdam University Medical Center, University of Amsterdam, Amsterdam, The Netherlands
[b] CLHC, Amsterdam Center for Forensic Science and Medicine, University of Amsterdam, Amsterdam, The Netherlands
[c] Netherlands Forensic Institute, Biological Traces, Den Haag, The Netherlands
[d] Department of Human Genetics, Genomics of Neurodegenerative Diseases and Aging, Vrije Universiteit Amsterdam, Amsterdam University Medical Center, Amsterdam, The Netherlands
[e] Delft Bioinformatics Lab, Delft University of Technology, Delft, The Netherlands
[f] Department of Anthropology, University of Amsterdam, Amsterdam, The Netherlands
[g] University of Amsterdam, Swammerdam Institute for Life Sciences, Amsterdam, The Netherlands
[h] Amsterdam Reproduction and Development research Institute, Amsterdam, The Netherlands
[i] Amsterdam Gastroenterology Endocrinology Metabolism, Amsterdam, The Netherlands

ARTICLE INFO

ABSTRACT

Introduction: The field of forensic DNA analysis has undergone rapid advancements in recent decades. The integration of massively parallel sequencing (MPS) has notably expanded the forensic toolkit, moving beyond identity matching to predicting phenotypic traits and biogeographical ancestry. This shift is of particular significance in cases where conventional DNA profiling fails to identify a single suspect. Supplementing forensic analyses with estimated biological age may be valuable but involves a complex and time-consuming DNA methylation analysis. This study explores and validates the performance of a comprehensive forensic third-generation sequencing assay utilizing Oxford Nanopore Technologies (ONT) in an adaptive and direct sequencing approach. We incorporated the most widely used forensic markers, i.e., STRs, SNPs, InDels, mitochondrial DNA (mtDNA), and two methylation-based clock classifiers, thereby combining forensic genetic and epigenetic analysis in one single workflow.
Methods and results: In our investigation, DNA from six anonymous individuals was sequenced using the ONT standard adaptive direct sequencing approach, reaching a mean percentage of on-target reads ranging from 6.6 % to 7.7 % per sample. ONT data was compared to standard MPS data and Illumina EPIC DNA methylation profiles. Basecalling employed recommended ONT software packages. *TREAT* was used for ONT-based analysis of autosomal and Y-chromosome STRs, achieving 90–92 % correct calls depending on allelic read depth thresholds. InDel analyses for two lower-quality samples proved challenging due to inadequate read depth, while the remaining four samples significantly contributed to the observed percentage markers (60.9 %) and correct calls (97.8 %). SNP analysis achieved a 98 % call rate, with only two mismatches and two missed alleles. ONT-generated DNA methylation data demonstrated Pearson's correlation coefficients with EPIC data ranging from 0.67 to 0.97 for Horvath's clock. Additional age-associated markers exhibited Pearson's correlation coefficients with chronological age between 0.14 (ELOVL2) and 0.96 (FHL2) at read depths of <30 and <20, respectively.

Despite excluding mtDNA from our targeted sequencing approach, adaptive proof-reading fragments covered the complete mtDNA with an average read depth of 21–72, showing 100 % concordance with reference data.

Discussion: Our exploratory study using ONT adaptive sequencing for conventional forensic and age associated DNA methylation markers showed high sequencing accuracy for a significant number of markers, showcasing ONT as a promising (epi)genetic forensic method. Future studies must address three critical aspects: determining clear quantity and quality measures and detection thresholds for accuracy, optimizing input DNA quantity for forensic casework expectations, and addressing ethical considerations associated with phenotype and ancestry analysis to prevent ethnic biases.

1. Introduction

In the late 1980s, molecular analysis applications revolutionized forensics, introducing DNA fingerprinting and later polymerase chain reaction (PCR) technologies. These advancements enabled robust identity matching in crime scene investigations, as well as paternity studies [28]. The integration of massively parallel sequencing (MPS) in the 21st century contributed to the elevation of the forensic toolkit beyond identity resolution, incorporating tools for phenotypic characterization and biogeographic origin [3].

Forensic DNA phenotyping (FDP) specifically focuses on predicting externally visible characteristics (EVCs) to generate a phenotype profile from crime scene samples. This aids investigations where perpetrator identity remains unknown based on conventional short tandem repeat (STR) DNA profiling [43]. For example, FDP proves valuable in cases without identified suspects and no matches in databases, as well as situations involving unidentifiable victims, helping to reconstruct physical characteristics of decomposed bodies [18]. Phenotype profiling reduces the victim or suspect pool, contributing to police investigations by prioritizing information in cases with conflicting statements or numerous leads [37,57]. Therefore, FDP has a significant role in contemporary forensic science. Nonetheless, the implementation of FDP in policing also comes with important ethical and societal challenges, since these technologies, by definition, cluster groups of people that become interesting for further policing, thereby introducing the risk of ethnic discrimination and stigmatization [45,57,58,80].

As per Kayser et al.'s (2023) review, FDP encompasses a combined evaluation of DNA-based predictions of biogeographical ancestry (BGA), physical traits, and biological age [43]. BGA determination involves distinct marker sets, including Y-chromosomal markers for paternal ancestry, mitochondrial DNA (mtDNA) for maternal ancestry, and autosomal markers for general ancestry. General ancestry informative markers (AIMs), e.g. autosomal insertions/deletions (InDels) [63] and single nucleotide polymorphisms (SNPs) [64], traditionally distinguish five continental groups, including Sub-Saharan Africa, Europe, East Asia, Native America, and Oceania Kayser et al., 2023; de la Puente et al., [15,43]. In addition, recent advancements include additional markers to further differentiate sub-populations [62,89,91]. X- and Y-chromosome markers facilitate familial research [72] and co-ancestry analysis in individuals with mixed backgrounds [74], while mtDNA offers insights into maternal ancestry and deconvolution of complex DNA mixtures [33]. Moreover, the high cellular copy number of mtDNA enhances the analysis of highly degraded trace samples [52]. Together, the three BGA components enhance BGA inferences in both females and males [12].

In addition to BGA, early forensic studies on physical appearance focused on identifying SNPs predictive for hair, eye, and skin color [11,83,84], resulting in the HIrisPlex-S prediction tool ($author1$ et al.,). However, because certain phenotypic traits (e.g., hair color) can be influenced by aging, it is important to complement physical appearance and BGA predictions with an age estimation. A common approach for determining biological age focuses on DNA methylation, an epigenetic feature where a methyl group is added to the $5'$ cytosine of C-G dinucleotides (CpGs) [2]. Methylation levels of specific CpGs are linked to age [42] and can be used to train DNA methylation classifiers, known as epigenetic clocks, which have been extensively studied in aging research [25,38,39,48,53,56]. The most widely used age estimator, developed by Steve Horvath in 2013, incorporates 353 age-associated CpGs identified in 51 different tissues [38]. In addition, The VISible Attributes through Genomics (VISAGE) Consortium created distinct forensic tools for predicting age in blood, buccal cells, bone tissue, and semen [29,65,88]. Several other studies identified age-predictive markers in teeth, hair, and nails [7,20,22,26], however, no validated tools for these markers exist so far [43].

Ideally, a comprehensive forensic genetic toolkit should integrate genetic identification with predictions of appearance, BGA, and biological age in a single assay. To this end, several commercial [41] and non-commercial [8,17,79,90] FDP tools exist that combine appearance and BGA markers. While these analyses have a similar workflow involving amplification and MPS readout, age prediction stands as a significant exception. For all the MPS-based age estimation tools mentioned above, detection of DNA methylation requires a bisulfite conversion step, necessitating a distinct sample processing and analysis procedure [76]. Therefore, combining genetic and epigenetic analyses in a unified assay demands an alternative sequencing approach.

Recent advancements in DNA research have led to direct long-read sequencing techniques, introduced by Oxford Nanopore Technologies (ONT) [66]. ONT devices employ a membrane with protein nanopores, guiding and analyzing DNA molecules. Each nucleotide passing through the pores causes distinctive disruptions in ionic current, which are translated into nucleotides using machine learning-based base calling algorithms [86]. Interestingly, the ONT algorithm is also able to detect modified bases [69,77], thereby enabling combined genetic and epigenetic analysis in a single assay. ONT sequencing can be applied to genomic DNA without complex processing, amplification, or bisulfite conversion [77]. Moreover, ONT's recently introduced adaptive sampling strategy enables real-time comparison of sequenced DNA molecules to pre-selected genomic target regions. Only 'on-target' molecules are fully sequenced, while 'off-target' molecules are ejected from the nanopores. This results in highly efficient selection and sequencing of target molecules. ONT devices have been previously used to analyze various FDP and forensic DNA markers, including STRs, SNPs, mtDNA, and epigenetic clocks [24,27,70,93], making it a promising tool for comprehensive FDP and DNA identification analysis.

In this proof-of-concept study, we aim to fully explore and evaluate ONT sequencing capabilities in a single, direct long-read sequencing assay, addressing frequently utilized DNA identification and (epi)genetic FDP marker sets in forensic science.

2. Methods

Sample selection and DNA extraction: We included DNA extracted from blood samples of six males aged 19–53 years at the time of sample collection. A detailed description of the sample cohort is presented in Table S1. Samples were anonymized and consent was obtained exclusively for technical optimization and validation purposes. This study refrains from disclosing genotype details concerning sample anonymity, and neither raw nor processed data is publicly accessible. As an alternative, Figs. S1–4 show IGV screenshots for a number of loci for all six samples. DNA was isolated from whole blood (EDTA) using FlexSTAR

workflow (AutoGen), conform manufacturer's protocol. DNA concentration was determined using the Qubit dsDNA BR assay using the Qubit Fluorometer (Invitrogen) according to manufacturer's instructions. Molecular weight distribution was evaluated using the Femto Pulse system (Agilent), following manufacturer's instructions.

Target selection: We included the following forensic DNA markers for ONT adaptive sampling and validation: 28 autosomal STRs, Amelogenin, 24 Y-STRs, and seven X-STRs (Verogen ForenSeq DNA Signature Prep Kit (Qiagen) and IDSeek OmniSTR Global Autosomal STR Profiling Kit (NimaGen)); 40 SNPs and 1 InDel of the HIrisPlex-S System [11,83, 84]; 46 ancestry predictive InDels as described by Pereira *et al* ([63]).; 8 DNA methylation markers previously reported by Wozniak *et al* ([88]). and 353 methylation markers previously reported by S. Horvath [38]; and the complete mtDNA mitogenome. A detailed overview of the selected markers and their genomic positions is provided in Table S2 and Supplementary File 1, respectively.

ONT sequencing and data-analysis procedures: All target regions, with exception of mtDNA, were defined in.bed files for adaptive sampling. Genomic positions for each marker were extended with a ~12.5 kb window upstream and downstream of the target locus to create the adaptive sampling regions, in total covering 15.7 Mb (0.49 %) of the human genome. DNA (150 μl, 26.6 ng/μl) was fragmented to 10 kb using a gTUBE (Covaris) according to manufacturer's instructions. Fragmented DNA was subsequently concentrated in a SpeedVac and resuspended in 48 μl water. Library preparation was performed according to Nanopore's genomic DNA by ligation protocol for the SQK-LSK114 kit. Libraries were quantified with Qubit dsDNA BR assay and 20 fmol was loaded on a MinION platform using a R10.4 flow cell. After 20 hours, flow cells were washed with EXP-WSH004 (ONT) and reloaded with another 20 fmol library. The latter wash and reloading step were performed twice, resulting in a 72-hour total run for all samples. Raw MinION signals were basecalled with guppy (v.6.1.5) applying the super high accuracy algorithm for modified bases (dna_r10.4.1_-e8.2_400bps_modbases_5mc_cg_sup) [87]. The resulting fastq and modified Binary Alignment Map (modBAM) outputs, containing the canonical and modified base calls, were used for all subsequent analyses.

STR analysis using TREAT: We evaluated the extent to which the ONT sequencing technology can be used for genotyping STRs commonly used in forensics (Supplementary File 1). Before analysis, sequencing data was aligned to the GRCh38 reference build using minimap2 (default parameters with the option *map-ont*) [50]. Genotyping of STRs was done using an adapted version of TREAT [78], a toolkit designed to genotype tandem repeats from long-read sequencing data. In short, this tool extracts the sequences spanning the tandem repeats of interest, and then identifies haplotypes based on the size of the tandem repeats using a clustering framework (Fig. S5). Sequences resembling each individual allele were then queried for the presence of forensics alleles based on the list of alleles in Supplementary File 2 of Hoogenboom *et al* ([34]).. We repeated the analysis using different thresholds for the minimum allelic coverage (3, 4, 5, and 6, respectively). We incorporated quality control by excluding STRs in cases of low coverage. We also excluded SE33, DYS522, DYS385a-b, and DYS389II from further analysis because the allele variants found in the MPS-based validation data (see below) were not present in the list of forensic alleles used for TREAT analysis, and TREAT therefore returned no allele call. Candidate alleles underwent further curation by scoring the most likely allele (based on the repeat number size and relative coverage), and by interrogating nearby SNPs. Curated alleles were validated using standard forensics procedures based on deep short read sequencing. Forensic STRs were regarded as matching only when all predicted alleles, for a given sample, matched the curated alleles. Finally, we evaluated the effect of GC content, STR size and allelic coverage on matching the curated alleles, using a linear mixed-effect model.

mtDNA analysis using FDSTools: FDSTools (v1.2.0) [35,36] was used for analysis of the complete mitogenome. Two FDSTools libraries were created containing the complete mitogenome in adjacent intervals of 25

nucleotides as targets: library A starting from position 1 and library B starting from position 11. For each interval, a minimal and maximal length of 10–50 nucleotides was used to filter out the majority of non-mtDNA reads. A minimal of 5 reads were used for calling the major variant of each interval. A consensus of the results of library A and B was used to determine the final mitotype.

To gain insight in existing sequencing errors, minor sequence variants were also investigated for each 25nt mtDNA interval with read depth for the major variant of at least 40 and summarized by the type of sequence difference with respect to the major variant. Observed minors were divided in categories of >10 % and 5–10 % of the read depth of the major (lower percentages were not analyzed in detail as they would often be represented by only 1 read).

InDel analysis using FDSTools: FDSTools (v1.2.0) [35,36] was used for analysis of 46 ancestry informative InDels [63]. InDel ranges were defined spanning each InDel (of 2–23nt in length) with multiple nucleotides at both sides and included in an FDSTools library. For each InDel, a minimum and maximum length of 10–50 nucleotides was used to filter out the majority of non-specific reads. Automated allele calling was performed using FDSTools samplestats with a 20 % min-pct-of-max (-m) threshold and optimized according to the evaluation of the following three different combinations of stringency settings, including the minimal number of reads per allele (-n) and the summed total allelic reads of a marker (-E): (i) min reads (-n) 2, min-allele-reads (-E) 6; (ii) min reads (-n) 3, min-allele-reads (-E) 8; (iii) min reads (-n) 4, min-allele-reads (-E) 10. The min-allele-reads (-E) threshold incorporates the summed total number of reads for each allele passing the criteria for the minimum number of reads, in order to minimize the chance of incorrectly calling a heterozygous sample as homozygous.

SNP analysis using Clair3: Reads that were fully sequenced in adaptive sampling were extracted with seqtk (v1.4-r122) and aligned to GRCh37 with minimap2 (v.2.17-r941) using ONT pre-sets [50]. The aligned reads were used as input for clair3 (v1.0.4) to call single nucleotide variants (SNVs) with ONTs provided model (r1041_e82_400bps_-sup_v420) [94].

Because of generally low read depths in the SNP dataset, we added an additional threshold concerning homozygote calls. We assumed an expected allele distribution of 50 %/50 % in our DNA samples. Given this assumption, the theoretical chance of missing one allele is reduced to less than 1 % for total read depths of 8 or more reads per locus ($P(8$ reads of allele 1 | 8 reads of allele 2$) = 0.5^8 + 0.5^8 \approx 0.0078$). Therefore, we classified homozygote calls with more than 8 reads as a true homozygote, and those with fewer than 8 reads as potentially missed heterozygotes.

DNA methylation analysis: Modified base counts (5mC) at CpG sites were aggregated from guppy's modBAM into a bedMethyl file by ONT's modbam2bed. From this bedMethyl file the on-target calls were extracted for further analyses. Reads for which ONT was unable to generate a modified or canonical base call were excluded, as well as reads not passing QC and base calls with alternative nucleotide modifications. ONT methylated fraction (further referred to as ONT beta value) was calculated by dividing the total number of methylated cytosines by the total number of methylated and unmethylated cytosines (which equals the read depth) for each CpG. Comparative analysis of Horvath CpGs (ONT beta value vs. Illumina EPIC beta value) was performed applying linear regression and Pearson correlation analyses. VISAGE CpGs were analyzed similarly, except ONT data was compared to chronological age as no EPIC validation data was available.

Acquisition of validation data sets: Evaluation and validation of the acquired ONT sequenced dataset was based on MPS procedures implemented in current forensic practice.

DNA variants were validated at the department of Biological Traces of the Netherlands Forensic Institute, using a multiplex PCR/MiSeq strategy (Illumina). Sample preparation for both the IDseek® OmniSTR™ Global Autosomal STR Profiling kit (Nimagen, the Netherlands) and the Verogen ForenSeq DNA Signature Prep Kit

(Qiagen, Germany) were performed according to manufacturer's protocols using approximately 1 ng of input DNA in the PCR and using MiSeq FGx for sequencing. FDSTools was used for data analysis [36]. Note that FDSTools involves an algorithm that annotates allele names, which comprises a different strategy compared to STR analyses using TREAT (see above). DNA quantification for reference analysis and mtDNA sequencing of the Control Region was performed as described in [21] using approximately 1000 copies of mtDNA in each of the two PCRs per sample. Subsequent sequencing and analysis were performed on the MiSeq FGx using standard procedures [36]. Sample preparation and analysis of the 46 ancestry predictive InDels, and the HIrisPlex-S, were performed as previously described by Pereira et al. ([63]). and Chaitanya et al. [11], respectively. Briefly, 1 ng DNA was used in PCRs per sample, followed by SnaPshot Minisequencing analysis using an 3500xL Genetic Analyzer (ThermoFisher Scientific). Subsequent data analysis was performed using Genemarker HID v2.9.8. (Softgenetics).

DNA methylation validation profiles were performed via the department of Human Genetics of the Amsterdam University Medical Center, using the Illumina HumanMethylation Infinium Methylation EPIC BeadChip array conform the manufacturer's protocol. Prior to hybridization, 1 µg DNA was bisulphite converted using the Zymo EZ DNAm™ kit (Zymo Research) conform the manufacturer's protocol. Raw intensity data files (.idat) were loaded in R (v4.1.1) and subsequently quality control was performed using MethylAid (v1.20.0) [87]. Principal component analysis (PCA) was performed to examine batch structure and confirmation of sex. Raw methylation indices were normalized using the funnorm function available under the minfi package (v1.40.0) [50]. The following probes were eliminated: probes with detection p-value > 0.1, probes located on the allosomes, probes involving any known genetic bias and probes that cross-react with other genomic regions. Horvath's clock classifier, available within the Methylclock package (v1.3.1) [78], was applied to estimate the biological age of the samples.

3. Results

3.1. Efficient enrichment of genomic target regions using Nanopore adaptive sampling

General characteristics of the six subjects, general performance of Illumina EPIC validation, and adaptive ONT sequencing are described in

Table 1
Sample characteristics and general ONT performance.

Sample-ID	PH1	PH3	PH6	PH7	PH11	PH15
Biological sex	Male	Male	Male	Male	Male	Male
Age (years)	35.3	19.1	27.6	23.4	43.8	53.1
Age-est. (years)	36.6	21.6	32.7	26.7	51.4	48.1
Age-delta (years)	1.3	2.5	5.1	3.3	7.6	−5.0
DNA input (µg)	6	1.7	2	6	6	3
Mean size (kb), (CV (%))	36 (52)	18 (78)	30 (53)	33 (56)	25 (70)	35 (58)
Library (ng/µl)	55.2	19.6	44.6	96.4	104	69.2
# pores	1546	1351	1356	1567	1523	1388
# reads per pore per hour	114	45	114	35	62	90
Mean (kb) ± SD (kb) of on-target reads	5.3 ± 5.3	6.5 ± 7.6	6.7 ± 4.2	7.7 ± 6.4	7.4 ± 5.4	7.2 ± 5.1
% reads on target	6.8	7.4	6.6	6.8	7.3	6.7
RatioGA	14.6	13.6	15.2	14.8	13.6	14.9

Age: chronological age at the time of sample collection. Age-est.: biological age estimates based on DNA methylation profiles and Horvath's clock classifier. Age-delta: difference of estimated age (Horvath's clock) minus chronological age. Mean size based on *Femtopulse* analysis, CV%: coefficient of variation (100 % indicates standard deviation equals the mean). % reads on target: percentage of total reads in adaptive sampling targets (= 1/RatioGA). RatioGA: total number of reads / total number of on-target reads (= 1/% reads on target).

Table 1. All samples passed EPIC quality control analyses (detailed description in Table S3). Based on EPIC age-estimation, biological age and chronological age differences ranged between 1.3 and 7.6 years. *Femtopulse* analysis showed a mean fragment size ranging from 18 kb (PH3) to 36 kb (PH1), and for both PH3 and PH11 a relatively large coefficient of variation (ratio of standard deviation to the mean) was observed, 78 % and 70 % respectively. As for Nanopore flow cell characteristics and sequencing, a total of 1351 (PH3) to 1567 (PH7) pores were available, and mean length of sequenced fragments ranged from 5.3 (PH1) to 7.7 kb (PH7). The number of reads per pore per hour was highly variable between samples, ranging from 35 and 45 for PH7 and PH3 respectively to 114 for both PH1 and PH6. The adaptive sampling strategy resulted in a total of 6.6–7.4 % on-target reads, and subsequent total Genomic/Adaptive ratios (RatioGA) of 13.6–15.2. A detailed overview of the Nanopore run report is presented in Table S4.

3.2. Evaluation of Nanopore performance on forensic autosomal STRs, Y-STRs, X-STRs and Amelogenin

The primary forensic toolkit for identity matching comprises STR analysis. We evaluated the extent to which ONT technology can reliably genotype forensic STRs across different thresholds for allelic coverage. After quality control based on allelic coverage and database matching, 51 regions and all individuals were kept for the analyses (Fig. 1). At allelic coverage ≥3, we found 90.3 % regions matching the validation data (187/207 observations across six samples). This proportion was 90.7 % at allelic coverage ≥4 (157/173 observations across six samples), 90.4 % at allelic coverage ≥5 (132/146 observations across five samples), and 92 % at allelic coverage ≥6 (103/112 observations across five samples).

A total of 20 mismatches were observed across all samples. The vast majority of discordant genotypes (90 %, N = 18) were the result of a loss of a repeat unit in the estimated allele compared to the validated allele: for example, the estimated genotypes reported TTTC [62] while the validated allele was TTTC [72] (see Fig. S6). One discordant observation (PH15 D3S1358) was the result of a repeat number gain in the estimated allele compared to validation data, and one discordant finding (PH7 D13S317) was the result of an allele dropout, which caused a heterozygous genotype to be erroneously called as homozygous. Furthermore, for the discordant genotypes, we checked retrospectively the presence of the validated allele in the data: in 20 % of the cases (N = 4 observations), the validated allele was not present in any of the reads, while in 80 % of the cases (N = 16 observations) the validated allele was present in at least one read, although with low frequency, causing the allele not to be prioritized.

Overall, we found that shorter STRs and higher allelic coverage were significantly associated with matching the validated allele (p = 3.65×10^{-37} and p = 4.88×10^{-5}, respectively), while the effect of GC content was not significant (p = 0.41).

3.3. Non-targeted analysis of the mitochondrial control region

Information on a person's identity, in particular the maternal lineage, can be obtained by analysis of the mtDNA. Because of mtDNA's relatively high copy number in all human cells, we omitted mtDNA as a target in our adaptive enrichment strategies to avoid overrepresentation of mtDNA in our dataset. This implied that the mtDNA readout was solely based on the proofreading reads (∼200–400 bp) and sporadically observed longer reads that escaped the adaptive sampling procedure. Despite the absence of any enrichment, we observed a larger read depth in all samples compared to the autosomal, allosomal, or DNA methylation readouts. We reached mean read depths ranging between 21 (PH7) and 72 (PH11) reads, resulting in complete coverage (1–16,569 bp) of the mtDNA (Fig. 2) in all individuals.

Although data on whole mitochondrial genomes were available, we focused on a smaller section, namely the hypervariable region in the

Allelic Coverage ≥3

Locus	PH1	PH3	PH6	PH7	PH11	PH15
CSF1PO	8		7/6		7/5	7/6
D10S1248	4/12		10/5		8/9	10/7
D12S391	6/8		8/11	4/3	7/4	15/3
D13S317	6/6		9/13	6	6/6	10/7
D16S539	7/7		12/7		7/5	8/5
D17S1301	7/7		10/10			13
D18S51						5/7
D19S433	7/7		8/5			3/10
D1S1656	8/6		18	6/3	7/7	
D20S482			9	7/5	9/4	6/8
D21S11	9/5		13/8			5/8
D22S1045	4/8		5/5		7	5/6
D2S1338	6/3	4/3	7/11		7/9	3/6
D2S441	8		7/4		5/4	9/8
D3S1358	13			4/6	18/3	
D4S2408	9/7	3/5	9/3	3/3	7	16/12
D5S818	7/9		7/8	3/4	14/6	9/6
D6S1043	7/9			5/5	9/11	
D7S820	11/10		21	15	7/4	7
D8S1179	10/6		8/9		5/7	8/4
D9S1122	13		20/3			6/4
FGA	10/7		16/4		4/8	10/5
PentaD	5/6		11/7			
PentaE	6/6		12/7		3/5	8/4
TH01	9/3				7/7	11/5
vWA	11/5		5/8			9/7
DYS19	8	3	7	7		9
DYS389I	10		10	4		9
DYS390	15		3	5		7
DYS391	6	3	9		12	3
DYS392			9	3	3	5
DYS437	11		11		6	5
DYS439	6		9	3	9	6
DYS448	9		7		5	10
DYS481	6		14	3	4	5
DYS505	7		5			10
DYS533	9		6			3
DYS549	7	4	7	4	10	13
DYS570	6		7		9	10
DYS576	6		5		5	9
DYS612			10		11	5
DYS635	10		11	3	7	6
DYS643	12		4	5	7	6
Y-GATA-H4	5		4	5	11	3
AmelogeninY	10		9	3		3
AmelogeninX	6		13	5	9	11
DXS10135			10	6	6	
DXS7132	3		6		9	6
DXS7423	5		4	4		3
DXS8378	7		5		6	4
HPRTB	9		8		8	11

Allelic Coverage ≥4

Locus	PH1	PH3	PH6	PH7	PH11	PH15
CSF1PO	8		7/6		7/5	7/6
D10S1248	4/12		10/5		8/9	10/7
D12S391	6/8		8/11		7/4	
D13S317	6/6		9/13		6/6	10/7
D16S539	7/7		12/7		7/5	8/5
D17S1301	7/7		10/10			13
D18S51						5/7
D19S433	7/7		8/5			
D1S1656	8/6		18		7/7	
D20S482			9	7/5	9/4	6/8
D21S11	9/5		13/8			5/8
D22S1045	4/8		5/5			5/6
D2S1338			7/11		7/9	
D2S441	8		7/4		5/4	9/8
D3S1358	13			4/6		
D4S2408	9/7					16/12
D5S818	7/9		7/8		14/6	9/6
D6S1043	7/9			5/5	9/11	
D7S820	11/10		21	15	7/4	
D8S1179	10/6		8/9		5/7	8/4
D9S1122	13					6/4
FGA	10/7		16/4		4/8	10/5
PentaD	5/6		11/7			
PentaE	6/6		12/7			8/4
TH01					7/7	11/5
vWA	11/5		5/8			9/7
DYS19	8		7	7		9
DYS389I	10		10	4		9
DYS390	15			5		7
DYS391	6		9		12	
DYS392			9			5
DYS437	11		11		6	5
DYS439	6		9		9	6
DYS448	9		7		5	10
DYS481	6		14		4	5
DYS505	7		5			10
DYS533	9		6			
DYS549	7	4	7	4	10	13
DYS570	6		7		9	10
DYS576	6		5		5	9
DYS612			10		11	5
DYS635	10		11		7	6
DYS643	12		4	5	7	6
Y-GATA-H4	5		4	5	11	4
AmelogeninY	10		9		7	
AmelogeninX	6		13	5	9	11
DXS10135			10	6	6	
DXS7132			6		9	6
DXS7423	5		4	4		
DXS8378	7		5		6	4
HPRTB	9		8		8	11

Allelic Coverage ≥5

Locus	PH1	PH3	PH6	PH7	PH11	PH15
CSF1PO			7/6		7/5	7/6
D10S1248			10/5		8/9	10/7
D12S391	6/8		8/11			
D13S317	6/6		9/13		6/6	10/7
D16S539	7/7		12/7		7/5	8/5
D17S1301	7/7		10/10			13
D18S51						5/7
D19S433	7/7		8/5			
D1S1656	8/6		18		7/7	
D20S482				7/5		6/8
D21S11	9/5		13/8			5/8
D22S1045			5/5			5/6
D2S1338			7/11		7/9	
D2S441						9/8
D3S1358	13					
D4S2408	9/7					16/12
D5S818	7/9		7/8		14/6	9/6
D6S1043	7/9			5/5	9/11	
D7S820	11/10		21	15		
D8S1179	10/6		8/9		5/7	
D9S1122	13					
FGA	10/7					10/5
PentaD	5/6		11/7			
PentaE	6/6		12/7			
TH01					7/7	11/5
vWA	11/5		5/8			9/7
DYS19	8		7	7		9
DYS389I	10		10			9
DYS390	15			5		
DYS391	6		9		12	
DYS392			9			5
DYS437	11		11		6	5
DYS439	6		9			
DYS448	9		7			10
DYS481	6		14			5
DYS505	7		5			10
DYS533	9		6			
DYS549	7		7		10	13
DYS570	6		7		9	10
DYS576	6		5		5	9
DYS612			10		11	5
DYS635	10		11		7	6
DYS643	12			5	7	6
Y-GATA-H4			5		11	
AmelogeninY	10		9		7	
AmelogeninX			13	5	9	11
DXS10135			10	6	6	
DXS7132			6		9	6
DXS7423	5					
DXS8378			5		6	
HPRTB	9		8		8	11

Allelic Coverage ≥6

Locus	PH1	PH3	PH6	PH7	PH11	PH15
CSF1PO			7/6			7/6
D10S1248					8/9	10/7
D12S391	6/8		8/11			
D13S317	6/6		9/13		6/6	10/7
D16S539	7/7		12/7			
D17S1301	7/7		10/10			13
D18S51						5/7
D19S433	7/7					
D1S1656	8/6		18		7/7	
D20S482						6/8
D21S11			13/8			5/8
D22S1045			5/5			5/6
D2S1338			7/11		7/9	
D2S441						9/8
D3S1358	13					
D4S2408	9/7					16/12
D5S818	7/9		7/8		14/6	9/6
D6S1043	7/9					9/11
D7S820	11/10		21	15		
D8S1179	10/6		8/9			
D9S1122	13					
FGA	10/7					
PentaD			11/7			
PentaE	6/6		12/7			
TH01					7/7	
vWA						9/7
DYS19	8		7	7		9
DYS389I	10		10			9
DYS390	15					
DYS391	6		9		12	
DYS392			9			
DYS437	11		11		6	
DYS439	6		9			9
DYS448	9		7			10
DYS481	6		14			
DYS505	7					10
DYS533	9		6			
DYS549	7		7		10	13
DYS570	6		7		9	10
DYS576	6					9
DYS612			10		11	
DYS635	10		11		7	6
DYS643	12				7	6
Y-GATA-H4					11	
AmelogeninY	10		9			
AmelogeninX			13		9	11
DXS10135			10	6	6	
DXS7132			6		9	6
DXS7423						
DXS8378	7				6	
HPRTB	9		8		8	11

colors:
- ONT and validation data match
- single repeat number loss
- single repeat number gain
- dropout of one allele for heterozygote
- ONT data does not meet allele call conditions

Fig. 1. Evaluation of ONT performance for forensic STRs: ONT and validation data comparison, including total read depth of the 1–2 reported alleles per locus. Overview of ONT performance on Amelogenin and 49 STRs that passed quality control, including 26 autosomal STRs, 18 Y-STRs, and five X-STRs. The four panels present the same results, but with increasing allelic coverage thresholds (minimal number of 3, 4, 5, or 6 reads per allele, autosomal homozygous loci require respectively 6, 8, 10, or 12 reads in total to reach the coverage threshold). The second row indicates sample ID (N = 6). Numbers in highlighted areas indicate total read depth of the 1–2 prioritized alleles per locus (one number for autosomal homozygous loci and X- and Y-chromosomal markers, and two numbers representing allele specific read depths for heterozygous loci). Highlight in green indicates a match between ONT and validation data. Highlight in red indicates a single repeat number loss, while highlight in yellow represents a single repeat number gain. Highlight in orange indicates a mismatch with validation data, for which ONT data reports a homozygous variant while the validation data reports a heterozygous variant. Highlight in grey represents loci for which no ONT call was reported because data did not meet allele calling thresholds.

control region (D-loop), located at 16,009–16,569 bp and 1–589 bp. Both ONT and validation mtDNA data were mapped and aligned against the revised Cambridge reference sequence (rCRS) [4,5]. In all samples we observed a higher average read depth in the control region compared to the whole mitochondrial genomes (Table 2). All called major variants for each position in the control region showed a 100 % concordance between ONT and validation data (Table 2). The total number of observed differences to rCRS ranged between 4 (PH6) and 17 (PH7). Although both classical and ONT sequencing approaches may produce inaccurate calling within homopolymer repeats, our results indicated no adverse sequencing effects in the D-loop region (Table 2).

In addition, the high read depth mtDNA subset encouraged further exploration of ONT's performance. We analyzed infrequent (minor) sequence variants in relation to heteroplasmy or technical variation, relevant within a forensic setting. In particular, we addressed infrequent single nucleotide substitutions, deletions, and duplications. Therefore, we established a 'minor variant' threshold, based on a total read depth of ≥40, 25 bp intervals, and the following two categories: (i) 5–10 %, and (ii) >10 % contributions of minor variant (compared to sum of read depth of major variant, i.e., 2–4 reads and >4 reads, respectively, if major read depth is 40). The vast majority of the observed infrequent variation involved single nucleotide deletions, comprising 86 % and 59 % of the aforementioned >10 % and 5–10 % minor variant contributions, respectively. In contrast, single-base insertion and substitution errors were observed at a substantially lower frequency (Table 3).

3.4. Accurate detection of ancestry informative InDels

In addition to the Y-chromosome and mtDNA markers, predictive information related to an individual's ancestry can be acquired using autosomal InDels. A total of 46 autosomal InDels, previously described by Pereira et al. [63], were involved in our adaptive strategy enrichment
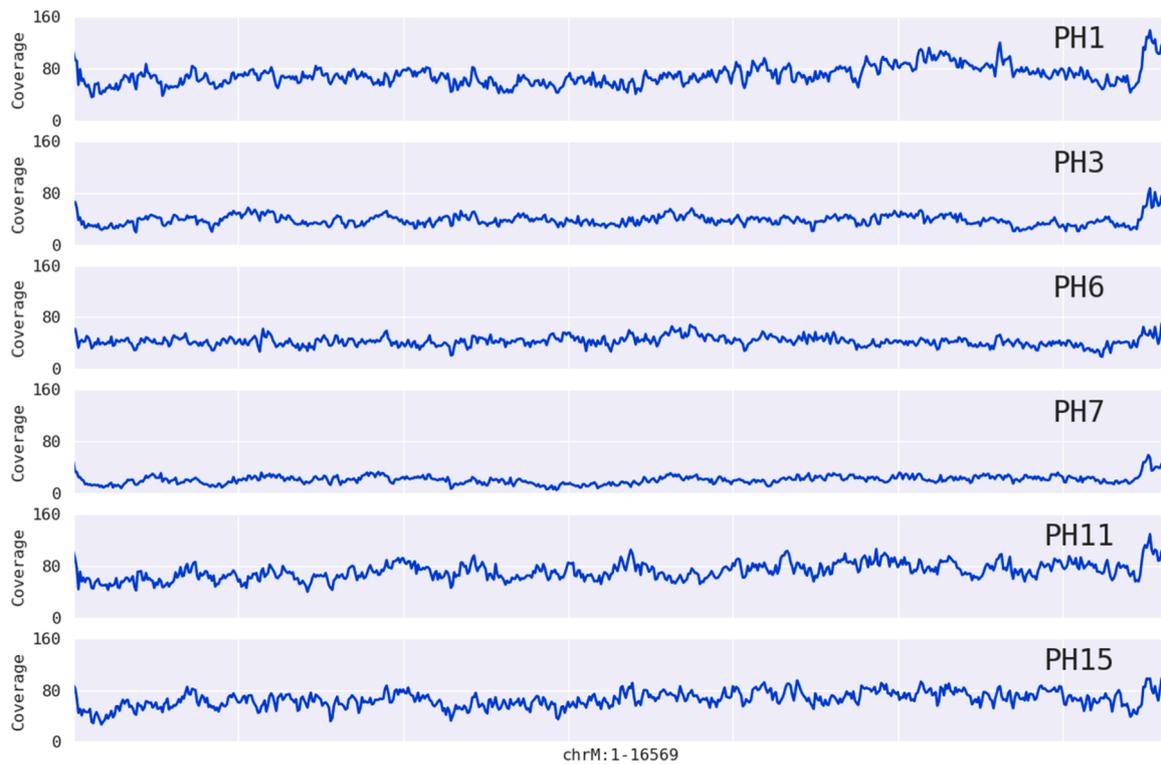
Fig. 2. mtDNA coverage plots per sample. The x-axis represents the complete mitogenome in adjacent intervals of 25 nucleotides, the y-axis represents read depth per interval (coverage).

Table 2

Average read depth per sample and total number of reported variants in D-loop compared to rCRS.

	PH1	PH3	PH6	PH7	PH11	PH15
Average read depth (full mtDNA)	70	38	43	21	72	66
Average read depth (D-loop)[1]	75	43	47	26	74	58
Observed differences from rCRS (total)	12	9	4	17	14	7
Observed differences ChrM:16,009-16,179	0	2	0	2	2	0
Observed differences ChrM:16,180-16,193 (C-stretch)	2	0	0	0	2	0
Observed differences ChrM:16,194-16,569 + 1-589	10	7	4	15	10	7

[a]Green highlight indicates a 100 % concordance of variants found in the ONT and validation data compared to rCRS.

Table 3

Distribution of observed errors in minor sequence variants.

Minor variant category	1 bp deletions	1 bp insertions	1 bp substitutions
5–10 %	86 %	5 %	9 %
>10 %	59 %	23 %	18 %

Table 4

Average InDel success rates for three different allele calling settings.

Allele calling settings			
Minimal reads per allele	2	3	4
Minimal total allelic reads	6	8	10
Minimal heterozygous balance	20 %	20 %	20 %
% called markers	74.6 %	60.9 %	42.8 %
% correct calls	98.4 %	97.8 %	97.8 %
% markers with allelic drop-out	1.1 %	1.8 %	1.4 %
Ratio of drop-ins / called alleles	0.11	0.03	0.03

procedure and subjected to validation using the MPS-acquired dataset. The number of bases varied among the studied InDels, ranging between two and 23 base pairs. Accurately identifying InDels is often hindered by inconsistent mapping events, resulting in variable start or end positioning of genetic variations. To overcome this, we used the standard MPS mapping and calling software, FDSTools, to call InDels from our ONT-generated dataset. This software package can reliably align InDels, as mapping is performed on the (invariant) regions flanking the target.

FDSTools allele calling options include settings such as the minimal number of reads per allele, minimal total allelic reads, and a minimum percentage in relation to the allelic balance. We evaluated a total of three distinct settings (Table 4), indicating a minimal number of three reads per allele and a minimal total number of eight reads in combination with a 20 % balance threshold as the most optimal settings. Using

these parameters, 60.9 % of the total number of markers could be characterized (N = 169), of which 97.8 % were called correctly. Finally, we observed allelic dropout occurring in 1.8 % of the total calls, and the ratio of the number of drop-ins compared to the total number of called alleles was minimized to 0.03.

Although we observed a relatively low average read depth among all samples, we noted no systematic drop out of InDels in our dataset (Fig. 3). We observed a substantial amount of missing data for the lower quality samples PH3 and PH7. In contrast, PH1 and PH15 showed no mismatches with the validation data, and only five and eight markers,

Fig. 3. Evaluation of ONT performance for ancestry predictive InDels: ONT and validation data comparison, including total read depth of the 1–2 reported alleles per locus. Overview of ONT performance on 46 ancestry predictive InDels, previously described by Pereira et al. [63]. Upper row indicates sample ID (N = 6). Numbers indicate total read depth of the 1–2 reported alleles per locus. Read depth per allele is not presented as this would reveal genotypes of sample donors. Highlight in green indicates matching ONT and validation data. Highlight in orange indicates mismatch with validation data, for which ONT data reports a homozygous variant while the validation data reports a heterozygous variant. Highlight in grey represents loci for which no ONT call was reported because data did not meet allele calling settings.

respectively, were excluded because they did not meet calling criteria. Although PH6 included the largest number of called InDels, this sample showed two allelic dropouts compared to validation data. Finally, for PH11 we observed a total of three allelic dropouts, while ten markers did not meet the calling criteria.

3.5. Efficient and robust detection of SNPs predictive of hair, eye, and skin color

We performed adaptive sampling of the regions encompassing all genetic variations included in the HIrisPlex-S assay, comprising 40 SNPs and 1 InDel that can be used to predict hair, eye, and skin color. Our enrichment approach yielded read depths ranging from 4 to 40 (Fig. 4). Due to the absence of a phasing strategy in our SNP analysis, we were only able to determine the allele coverage ratio (ACR) for heterozygous SNPs. To protect donor privacy, we have not presented allele-specific read depths, as doing so could potentially disclose individual genotypes. Instead, we used the heterozygous SNP positions to calculate the mean ACR and its standard deviation for each sample, varying from 0.61 for PH15 to 1.10 for PH1 (Table 5).

Overall, 98.4 % of the targeted forensic SNPs aligned with validation data (240/244 observations across six samples). Notably, for PH3, seven targets (rs683, rs1126809, rs1800414, rs12441727, rs1129038, rs3212355, and rs6119471) matched the validation outcome as homozygous reference variants but failed to meet our additional threshold of ≥ 8 reads (Fig. 4). Excluding these observations to improve data reliability resulted in an adjusted accuracy of 98.3 % (233/237 observations). A total of four discordant allele calls were observed across all samples, including two allelic dropouts (PH1 rs8051733 and PH3 rs28777), and two instances where ONT reported heterozygous variants, while the validation indicated homozygous reference alleles (PH3 rs1805005 and PH15 rs1805005).

3.6. Evaluation of nanopore performance on forensic age-predictive methylation markers

Next, we addressed the detection of DNA methylation in relation to biological age. A total of 353 age informative CpG targets present in the Horvath's clock were successfully incorporated into our ONT adaptive workflow. 334 of these loci are also present in the Illumina EPIC array used for technical validation [55], and were incorporated in our comparative analysis of ONT and validation data. General data evaluation showed that for a total of 39 CpGs (<12 %), no ONT data were generated or the data failed to pass quality control (Fig. 5). In addition, we observed a variable number of CpGs expressing beta values of 0 or 1 in all samples, ranging between 46 % and 74 % with respect to the total number of CpGs studied in each sample (Fig. 5). Notably, the total number of CpGs expressing a methylation value of 0 or 1 was negatively associated with read depth (Table S5). Since we achieved a relatively low maximum read depth of 29 for Horvath and VISAGE methylation targets, we excluded CpGs with beta values of 0 or 1 from our dataset and from subsequent comparative analyses. Of the remaining targets, a total of 23 CpGs were present across all samples.

Contrary to STR, InDel, and SNP variants, DNA methylation is

Table 5
Mean ACR and standard deviation per sample for all heterozygous HIrisPlex-S SNP positions.

Sample	Heterozygous SNPs	Mean ACR	ACR st.dev.
PH1	9	1.1059	0.4266
PH3	11	0.7950	0.7212
PH6	6	0.9652	0.3679
PH7	8	0.9227	0.5878
PH11	7	1.0603	0.4339
PH15	5	0.6168	0.2498

ACR: allele coverage ratio.

reported as a continuous variable. Therefore, we compared ONT methylation levels with those obtained from the classical Illumina EPIC array, using correlation analyses (Fig. 6). Correlations were presented according to three total read depth thresholds: (i) <10 reads, (ii) 10–19 reads, and (iii) 20–29 reads. All samples showed positive linear correlations between ONT and EPIC-generated data that generally increased with higher read depths, with a nominal exception for sample PH1. PH7 reached the lowest Pearson's correlation coefficient of 0.672 at read depths <10, covering a total of 78 CpG sites (Fig. 6 and Table S6). In contrast, the highest Pearson's correlation was observed in PH6 (0.976), at a read depth varying between 19 and 29 reads, covering 25 CpGs in total (Fig. 6 and Table S6).

In addition to Horvath's clock, we implemented CpGs previously reported by the forensic VISAGE Enhanced Tool for Age Prediction. We analyzed ONT-obtained beta values for six blood-specific age-predictive CpGs comprising the genes *MIR29B2CHG*, *FHL2*, *TRIM59*, *ELOVL2*, *PDE4C*, and *KLF14*. Most VISAGE targets are not included in the Illumina EPIC array, hampering a direct comparison between ONT and validation datasets. Therefore, we correlated ONT beta values to chronological age instead (Fig. 7). *KLF14* was excluded due to a reported ONT beta value of 0 for all samples, despite read depths varying from 5 to 17 per sample (data not shown). *MIR29B2CHG* showed an expected negative correlation with age (R = −0.92). *FHL2* and *TRIM59* showed a positive correlation with chronological age of R = 0.96 and R = 0.75 respectively. All three markers included both low and medium read depths per CpG site. For *ELOVL2*, we observed a large variation in beta values and no correlation (R = 0.14) between ONT generated beta values and chronological age, despite medium to high read counts per target CpG. Finally, *PDE4C* showed a correlation of R = 0.86 with chronological age, including an equal distribution of low and medium reads per CpG site.

4. Discussion

Summary: In this study, we explored the performance of direct and adaptive ONT sequencing in a forensic context. We assessed commonly used markers, including STRs, SNPs, InDels, mtDNA, and two DNA methylation-based clock classifiers for identity matching and Forensic DNA Phenotyping (FDP) analysis.

We observed variable performance across the samples, which was most likely a result of flow cell pore efficiency. Comparison of ONT data with validation datasets indicated overall good accuracy for all marker types, albeit with abundant missing data under stricter quality parameters, especially for STRs, InDels, and CpGs. The continuous nature of DNA methylation was particularly challenging due to low read depths. However, after extensive quality control, our ONT dataset reached high correlations with classical array-based DNA methylation data or chronological age.

This study promotes ONT direct sequencing for future forensic applications. Further research should focus on enhancing on-target read depths, innovating new approaches to decrease input DNA quantity or even use degraded DNA, and expanding molecular classifiers, particularly for phenotypic characterization.

Application of PCR-free ONT sequencing in forensics: To the best of our knowledge, this explorative study on Nanopore sequencing is the first in a forensic context to directly employ fragmented DNA for adaptive sampling of both forensic STRs and a comprehensive set of genetic and epigenetic FDP markers in an all-in-one and PCR-free approach. This diverges from other recent reports, all using PCR steps during sample or library preparation prior to ONT sequencing [10,51].

We assumed that data output quality of our approach hinges on two primary factors: the quality and quantity of DNA samples, and the technical specifications of the ONT platform and flow cells. Extensive DNA quality control revealed that two samples (PH3 and PH11) had smaller average fragment lengths and larger variations in DNA fragment size, indicating lower sample integrity. To correct for this, we used DNA fragmentation (up to 10 kb) and adjusted library concentrations to

	PH1	PH3	PH6	PH7	PH11	PH15
rs16891982	40	9	26	9	13	15
rs28777	31	12	21	17	14	21
rs12203592	21	12	18	12	22	22
rs4959270	33	15	26	9	14	24
rs683	25	6	22	15	14	21
rs10756819	20	14	23	20	16	17
rs1042602	27	15	12	9	20	15
rs1393350	24	15	18	17	15	22
rs1126809	21	6	16	13	16	17
rs12821256	29	12	16	14	21	18
rs12896399	27	10	27	14	16	30
rs2402130	23	15	18	15	15	15
rs17128291	34	9	23	12	19	23
rs1545397	20	7	21	11	18	24
rs1800414	20	5	8	7	15	28
rs1800407	19	13	16	16	16	14
rs12441727	28	6	12	7	15	17
rs1470608	24	8	23	14	11	23
rs1129038	19	7	18	16	21	23
rs12913832	29	10	11	16	18	29
rs2238289	22	7	26	12	9	14
rs6497292	28	10	19	8	13	21
rs1667394	12	10	19	14	19	18
rs1426654	24	5	22	13	14	28
rs3114908	24	9	22	4	15	14
rs3212355	23	5	17	9	9	12
rs1805005	27	9	17	11	10	12
rs1805006	27	9	17	11	10	12
rs2228479	27	9	17	12	10	12
rs11547464	27	9	17	13	10	12
rs1805007	27	9	17	13	10	12
rs201326893	27	9	17	13	10	12
rs1110400	28	9	17	13	10	12
rs1805008	28	9	17	13	10	12
rs885479	26	9	17	13	9	12
rs1805009	28	9	19	13	10	12
rs8051733	13	7	20	12	14	31
rs796296176	26	9	17	11	10	12
rs6059655	15	19	17	14	12	17
rs6119471	28	7	17	13	18	12
rs2378249	32	12	16	12	17	14

Colors:
- ONT and validation data match
- Drop out of one allele for heterozygote
- Heterozygous ONT call while homozygous validation data
- ONT data does not meet homozygote threshold (≥8 reads)
- No validation data available

Fig. 4. Evaluation of ONT performance for HIrisPlex-S SNPs: ONT and validation data comparison, including total read depth of the 1–2 reported alleles per locus. Overview of ONT performance on the HIrisPlex-S panel, including 40 SNPs and 1 InDel (rs796296176). Upper row indicates sample ID (N = 6). Numbers indicate total read depth of the 1–2 reported alleles per locus. Read depth per allele is not presented as this would reveal genotypes of the sample donors. Highlight in green indicates read depth ≥8, with no mismatch according to the validation data. Highlight in orange indicates mismatch with validation data, for which ONT data reports a homozygous variant while the validation data reports a heterozygous variant. Highlight in purple indicates mismatch with validation data, for which ONT reports a heterozygous variant while the validation data reports a homozygous variant. Highlight in grey indicates no mismatch with the reported homozygous reference call in the validation data, but with ONT read depth <8.

ensure equal loading of molecules per sample on each flow cell, although low-integrity samples were likely enriched with shorter fragments (<10 kb) due to additional fragmentation.

ONT's technical factors, such as pore availability and efficiency, may impact data quality by affecting total coverage and read depths. In this study, pore availability was similar across flow cells. In contrast, pore efficiency, as measured by average reads per pore per hour, was notably

low for PH3 and PH7.

Global evaluation of ONT adaptive sampling, including average read length, percentage of on-target reads, and enrichment value (G/A ratio), revealed minimal variation between samples and flow cells. However, as discussed in the data evaluations below, consistently low performance was indicated particularly in PH3 but also in PH7. This suggests that pore efficiency, rather than DNA integrity (as represented by fragment
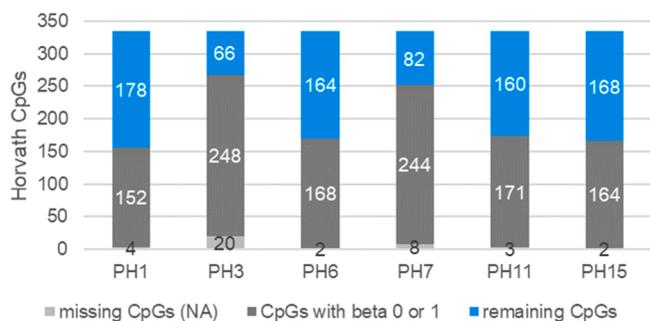
Fig. 5. General data exploration of ONT DNA methylation data (Horvath's clock). General presentation of missing CpGs, CpGs with beta value 0 or 1, and remaining CpGs, presented per sample.

length distributions), influences sequencing output. Since we did not include replicates in our study, we were unable to further evaluate the impact of poor sample quality and variable quality of the flow cells separately. Nevertheless, this exclusion of the possibility that DNA integrity affects sequencing performance aligns with reports from others, which have shown that long to very long DNA fragments are particularly prone to clogging events, which in turn decrease pore sequencing efficiencies [14,46].

STRs: The analysis of 59 STRs (28 autosomal, 24 Y-chromosome, and seven X-chromosome) yielded >90 % matching genotypes across 51 markers observed in at least one sample. Interestingly, we achieved this with as little as ≤28 reads per locus. Other studies using ONT devices for STR analyses report similar or slightly better results. Hall et al. [24] reach a 100 % accuracy for autosomal STRs using STRspy as base calling method, while Tytgat et al. [81] report high concordance for autosomal STRs and a 100 % accuracy for Y-STRs using Guppy as a base caller. However, both studies use amplicon-based libraries, resulting in total read depths of >100k and >212 respectively.

Evaluation of allele-specific read depths for autosomal heterozygous loci showed imbalances across all samples. However, we found only one allele dropout event (PH7/D13S317) at the least strict allele coverage threshold of ≥3. These results suggest that sufficient read depths, in combination with a coverage threshold of at least 4 reads, mitigate the effects of allelic imbalances.

The observed discordances were clearly not randomly spread across different markers: higher allele size as well as lower coverage were significantly associated with discordant calls, indicating that specific markers are more sensitive to errors. Increasing the allelic threshold to ≥4 removed discordant genotype calls in three markers (D13S317, D3S1358, DYS485). However, three other markers (FGA, D18S51, DYS570) consistently yielded incorrect calls across all samples, while five markers (D2S1338, PentaD, DYS576, DYS612, DXS10135) showed persistent discordances despite improved quality parameters.

The majority (90 %) of observed mismatches in our ONT STR dataset concerned repeat number loss of a single tandem repeat. These backward (or −1) stutter effects are often observed in forensic STR analysis, especially in MPS readouts, and as a result also in subsequent amplicon based ONT datasets [24,71]. Interestingly, we observed stutter effects despite omitting any amplification steps, potentially hinting at issues with Nanopore base calling algorithms in handling repetitive sequences. Alternatively, since Nanopore sequencing allows for analysis of individual DNA molecules instead of amplicons, the observed repeat number loss may also reflect biological somatic variability, rather than technical sequencing errors.

Incorporating the highly polymorphic STR SE33 into our adaptive approach posed challenges due to its extreme heterozygosity. Despite being one of the most informative forensic markers [9], amplicon-based sequencing of SE33 faces many challenges such as allelic dropouts [30, 32] and discordant genotype calls [73,85]. Nanopore could offer an alternative primer and amplification-free sequencing approach for this

locus. However, in this study we were unable to analyze SE33, as well as DYS522, DYS385a-b, and DYS389II because a non-comprehensive list of markers and corresponding reference alleles was used in our TREAT analysis, and the alleles observed in the MPS-based validation data were not present in this reference list. For all other markers, all validated alleles were present in the aforementioned list, indicating that any missing markers for a particular sample can be attributed to low read depth. For future research, integrating the STRNaming nomenclature [36], which we also used for generating our MPS-based validation data, would allow for algorithm based allele calling, eliminating the need for a pre-existing list of allele variants and simplifying the comparison of ONT and MPS data.

For identity matching in a forensic context, the total number and discriminative power of reported autosomal loci determines the evidentiary value of DNA samples. Our study reveals that under the strictest criteria of ≥6 reads per allele, two samples (PH1 and PH6) showed accurate genotypes for 13 markers, except for FGA for PH1. Interestingly, lowering the threshold to ≥3 reads per allele expanded this number to 22 markers for PH1 (excluding mismatches for FGA and PentaD) and 21 markers for PH6 (excluding a mismatch for FGA), as well as included PH11 with 17 markers (excluding mismatches for D2S1338 and FGA), and PH15 with 22 markers (excluding mismatches for D18S51, D3S1338, and FGA). Overall, with the least strict parameters (≥3 reads per allele) and with the exception of missing data, we correctly called 20 autosomal STRs across all samples. With further optimization to detect inaccurate variant calls, we expect that ONT could in the future be a viable tool for forensic identity matching.

mtDNA: In the present study, we purposefully excluded mtDNA from the adaptive enrichment approach, assuming that adaptive proofreads would provide sufficient coverage of the entire mtDNA. Our results showed higher read depths for mtDNA, particularly in the hypervariable region (D-loop), compared to autosomal markers. Importantly, no sequence discordances were observed, indicating the accuracy of ONT direct sequencing at read depths of 26–75 reads. Our results are in line with Zascavage *et al.*, who reported high sequencing accuracy for mtDNA at an average coverage of 15–92 reads per sample using a PCR-free Nanopore sequencing approach [93]. Notably, despite large differences in total read coverage, their results demonstrate comparable accuracy between PCR-free and PCR-enriched libraries [93], indicating ONT as a promising direct and low-coverage sequencing technology.

InDels: In our adaptive sampling approach, we analyzed a total of 46 ancestry-informative autosomal InDels [63] using the FDSTools software package designed for short read MPS data [35,36]. Among the 60.9 % called markers, we reached 97.8 % accuracy. Here, discordant sequence variants with validation data were observed only in sample PH6 and PH11, missing two and three alleles, respectively.

We generally observed a lower read depth for InDels compared to SNP analysis, primarily due suboptimal alignment events. Such events are not only a challenge in long read sequencing but may also be observed in short read MPS experiments [49]. Furthermore, for InDel detection we utilized three distinct quality parameters. We found that stricter thresholds, such as increasing the minimum read per allele and total allelic reads, neither enhanced the accuracy of calls nor substantially decreased drop-out and drop-in events. Salakhov et al. recently documented pathogenic variant detection using older ONT sequencing technology and long PCR fragments [75]. They noted decreased accuracy in InDel calling due to heightened deletion/insertion errors. Likewise, Maestri et al. demonstrated reliable and efficient calling of single nucleotide variants, but not InDels, using direct long read ONT sequencing for haplotype reconstruction [54].

To our knowledge, no specific study has assessed InDel calling performance using the latest direct ONT sequencing methodology (R10.4.1. and software) [87]. Future experiments should explore whether alternative calling tools could enhance InDel detection in datasets generated by direct ONT sequencing. For instance, Abdelwahab et al. previously investigated AI-based variant callers, highlighting their variable
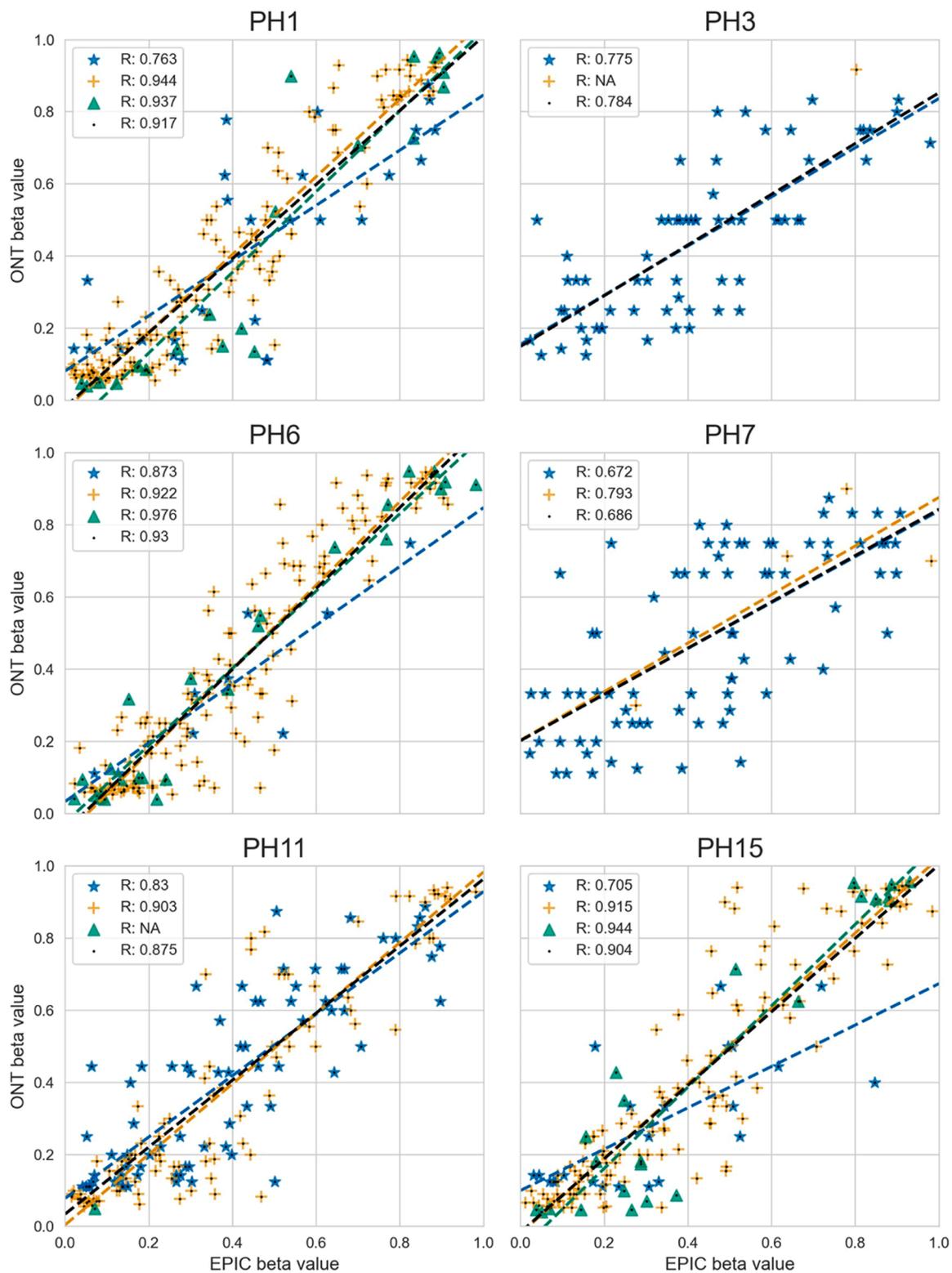
Fig. 6. Correlation plots showing linear regression between ONT and validation DNA methylation data (Horvath's clock). The y-axis shows beta values as measured with ONT; the x-axis shows beta values as measured in the EPIC validation data set. Each data point represents one locus. Small black dots include all loci per sample. Blue star-shaped dots indicate loci with a read depth <10. Orange plus-shaped dots represent loci with a read depth of 10–19. Green triangular dots indicate loci with a read depth of 20–29. Dotted lines show linear regression (black = all loci, blue = read depth <10, orange = read depth 10–19, green = read depth 20–29). R values represent Pearson's correlation coefficient.
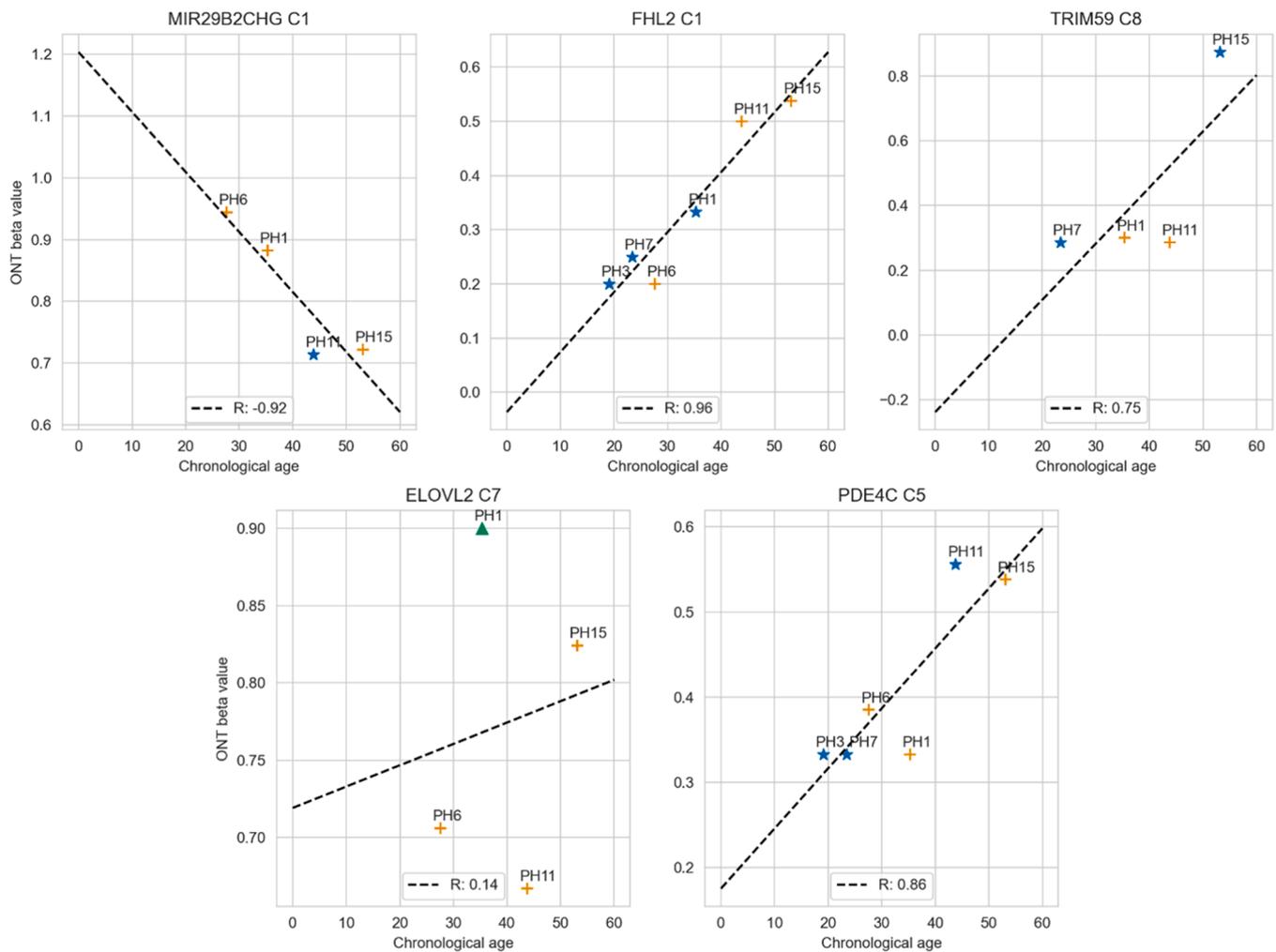
Fig. 7. Correlation plots showing linear regression between ONT DNA methylation data and chronological age (VISAGE Enhanced Tool for Age Prediction). Each panel represents a target predictive of age in blood as reported by Wozniak et al. [88]. A detailed overview of exact genomic positions per CpG is presented in Supplementary File 1. KLF14 was excluded due to a reported ONT beta value of 0 for all samples. The y-axis shows beta value as measured with ONT; the x-axis shows chronological age. Each dot represents one sample. Colors and symbols indicate read depth (blue star = low read depth of <10, orange plus = medium read depth of 10–19, green triangle = high read depth of 20–29). Black dotted line shows linear regression of all loci for each target. R value represents Pearson's correlation coefficient.

accuracy across different sequencing platforms [1].

SNPs: We integrated the HIrisPlex-S panel in our forensic ONT assay, comprising 40 SNPs and 1 InDel predictive of hair, eye, and skin color [11,83,84]. Using Clair3 with default settings as variant caller, we achieved an overall accuracy of 98 %, which is comparable to accuracies observed in other studies on ONT-based SNP analyses [6,31]. Furthermore, we confirm the accuracy of Clair3 for ONT sequencing data with low read depth (maximum of ≤40 reads) [94].

Our SNP dataset included four discordant sequencing calls. Two discordances resulted from allelic dropout, while the other two involved rs1805005, where Clair3 reporting a heterozygous variant for ONT data while validation data indicated homozygous reference alleles. Our results are similar to Tytgat *et al* ([81])., who reached a 99 % accuracy for SNP genotyping of amplicon libraries using Nanopore sequencing. Moreover, our results were based on ≤40 reads per SNP locus, compared to 60,049 ± 27,124 and 50,441 ± 27,985 basecalled reads per sample as reported by Tytgat *et al* ([81])., using Guppy and Bonita as basecallers, respectively.

Evaluation of the ACR showed an imbalance in allele coverage, particularly in PH3 and PH15, likely due to the two incorrect heterozygous calls in these samples. While we recommend incorporating ACR analysis as a standard quality control measure, our findings suggest that

the impact of imbalanced ACR is mitigated when sufficient read depths are achieved.

DNA methylation: In addition to genetic markers, we incorporated epigenetic DNA methylation markers indicative of biological age, including 353 age-associated methylation markers of Horvath's clock [38]. Our adaptive sampling strategy resulted in a maximum of ≤29 reads per target. Comparison of the 334 Horvath markers present in both ONT and EPIC datasets showed a general increase in Pearson's correlation coefficient with rising read depths.

Additionally, we included six forensic age predictive CpGs in blood from the VISAGE Enhanced Tool for Age Prediction [88]. As no validation data was available, ONT data was compared to chronological age. Similarly to Wozniak *et al.*, our data showed a positive correlation with age for *FHL2*, *TRIM*59, *ELOVL2*, and *PDE4C* and a negative correlation for *MIR29B2CHG* ([88]). Notably, ELOVL2 displayed a very low Pearson's correlation coefficient. Other studies show that *ELOVL2* is highly associated with age [59,88], and further studies are required to explain the deviating results for this marker in our dataset. Despite this outlier, all other markers exhibited relatively high correlations with chronological age.

Our study, including only four to six data points per VISAGE marker, demonstrates the resilience of these loci's age correlating properties

even with small sample sizes. This differs from Yuen et al.'s findings, who used ONT direct sequencing and adaptive sampling for analyzing VISAGE aging markers in ten human blood samples. While they found similar or higher correlations between ONT data and chronological age for *MIR29B2CHG* and *ELOVL2*, respectively, their correlations for *FHL2*, *TRIM59*, *KLF14*, and *PDE4C* were <0.675 [92]. Unlike Yuen *et al.*, we meticulously cleaned our DNA methylation dataset by removing loci reporting 0 % or 100 % methylation levels. We argue that the continuous nature of DNA methylation data in combination with low read depth resulted in unreliable results at the methylation extremities. Although our cleaning step resulted in substantial data loss, our results suggest that increasing the read depth for DNA methylation targets could reduce the amount of extreme and probably inaccurate methylation observations, thus improving correlations between ONT data and chronological age.

Limitations: While this study presents promising findings, we acknowledge a number of limitations. Firstly, there was variability in both the quality and quantity of DNA across the samples. As previously noted, the absence of replicates in our study precluded a separate evaluation of the impact of poor sample quality versus variable flow cell quality. Additionally, the quantity of input DNA (1.7–6.0 µg) was far from realistic for forensic case studies. Exploring the use of lower input material in our sequencing approach is a necessary consideration for future experiments.

Secondly, the use of standard MinION R10.4 flow cells and their associated pore resolution resulted in low target read depths, despite employing ONT's adaptive sampling strategy. This led to considerable loss of data for mainly STRs, InDels, and CpGs, especially with stricter quality thresholds. Optimization of calling software packages for each marker type is required to improve data accuracy and reliability, especially for low-coverage datasets. This is further substantiated by the minor variant analysis we performed on our high coverage mtDNA subset. Here, we observed a notable amount of single base deletions, and to a lesser extend single base insertions and substitutions. InDel biases with regard to ONT sequencing were also reported by others [16,40,44], underscoring the necessity for properly validated detection limits or threshold values before any of the described analyses can be implemented in forensic practice.

Future perspectives and recommendations: Follow-up studies on direct and adaptive ONT sequencing within a forensic context should address numerous aspects, including technology performance, extension of marker sets, and ethical considerations.

To enhance performance, future studies could explore employing a larger ONT platform, such as PromethION, which offers five times the pore count compared to MinION. This augmentation theoretically translates to a fivefold increase in read depth and more accurate results for all marker types. In addition, PromethION's enhanced sequencing efficiency and robustness, attributed to better operational control, present a notable advantage over MinION, particularly in mitigating external factors like temperature variations. Moreover, addressing the inherent challenges of direct sequencing, such as random fragment generation, necessitates optimization of all data analysis components, including base calling, alignment, and variant identification. Developing or refining algorithms tailored for direct sequencing and integrating larger datasets are crucial avenues for improving sequencing outcomes and forensic applicability. Finally, adding replicates would significantly enhance the reproducibility of the study and allow for distinct evaluation of the effects of sample and flow cell quality.

Regarding the extension of marker sets, future studies could integrate numerous additional genetic and epigenetic classifiers. For example, hair-related traits such as shape, baldness, greying (combined with age), and eyebrow color can be estimated using a relatively small number of single nucleotide variants [13,23,61,67,68]. Additionally, recent studies on body fluid identification report a small number of DNA methylation markers useful in discerning blood from semen and saliva specimens [47,60]. Integrating these markers in our adaptive workflow

is highly feasible, as adjustments in target region size allow for incorporating more enrichment targets. However, additional classifiers should be implemented with caution, as data analysis and interpretation tools for these markers may not yet be readily available or thoroughly validated for forensic applications.

Finally, the use of ONT platforms could revolutionize FDP analysis, accelerating the forensic process by providing investigative leads into the identity of unknown suspects. However, since such leads point towards ethnically defined groups rather than individuals, precautionary steps must be taken to prevent stigmatization. The cautious conduct followed in the Dutch Milica van Doorn case might be instructive here [82]. Additionally, ethnicity is known to impact DNA methylation based age predictions [19], underscoring the importance of properly training FDP prediction tools to mitigate ethnic biases.

5. Conclusion

Our study, exploring direct ONT sequencing in the context of an adaptive enrichment strategy for a broad scope of forensic markers, indicated promising but not yet flawless results. We integrated genetic and epigenetic classifiers for identity matching, phenotypic traits, ancestry, and biological age into a single workflow, highlighting ONT's potential as a rapid and efficient forensic sequencing tool. However, further optimizations are needed before ONT can be effectively implemented and accepted within the forensic field. These include addressing technical challenges, such as ensuring sufficient read depths, especially in combination with low DNA input. Additionally, refining the performance of variant calling algorithms is essential to enhance the accuracy of STRs, SNP, InDel, mtDNA, and DNA-methylation calling. Despite these challenges, our study presents proof-of-concept for future adaptation of ONT adaptive sampling as a comprehensive forensic sequencing assay for multiple forensic analyses.

CRediT authorship contribution statement

Titia Sijen: Writing – review & editing, Writing – original draft, Conceptualization. **Marcel J.T. Reinders:** Writing – review & editing, Methodology. **Amade Aouatef M′charek:** Writing – review & editing, Writing – original draft. **Jerry Hoogenboom:** Writing – review & editing, Methodology, Formal analysis. **Natalie E.C. Weiler:** Writing – review & editing, Formal analysis. **Peter Henneman:** Writing – review & editing, Writing – original draft, Methodology, Conceptualization. **Martin A. Haagmans:** Writing – review & editing, Writing – original draft, Visualization, Methodology, Formal analysis, Conceptualization. **Kristiaan J. van der Gaag:** Writing – review & editing, Writing – original draft, Visualization, Methodology, Formal analysis, Conceptualization. **Yaran Zhang:** Writing – review & editing, Methodology. **Henne Holstege:** Writing – review & editing, Methodology. **Niccoló Tesi:** Writing – review & editing, Writing – original draft, Visualization, Methodology, Formal analysis. **Alex N. Salazar:** Writing – review & editing, Methodology. **Desiree D.S.H. de Bruin:** Writing – review & editing, Writing – original draft, Visualization, Methodology, Formal analysis, Conceptualization.

Funding

Declaration of Competing Interest

The authors declare that they have no known competing financial interests or personal relationships that could have appeared to influence the work reported in this paper.

Appendix A. Supporting information

Supplementary data associated with this article can be found in the online version at doi:10.1016/j.fsigen.2024.103154.

References

[1] O. Abdelwahab, F. Belzile, D. Torkamaneh, Performance analysis of conventional and AI-based variant callers using short and long reads, BMC Bioinforma. 24 (1) (2023) 472.

[2] Alberts B., Johnson A., Lewis J., Morgan D., Raff M., Roberts K., Walter P. Molecular Biology of the Cell. New York: Garland Science; 2015.

[3] S.M. Aly, D. Sabri, Next generation sequencing (NGS): a golden tool in forensic toolkit, Arch. Med Sadowej Kryminol. 65 (4) (2015) 260–271.

[4] S. Anderson, A.T. Bankier, B.G. Barrell, M.H. de Bruijn, A.R. Coulson, J. Drouin, et al., Sequence and organization of the human mitochondrial genome, Nature 290 (5806) (1981) 457–465.

[5] R.M. Andrews, I. Kubacka, P.F. Chinnery, R.N. Lightowlers, D.M. Turnbull, N. Howell, Reanalysis and revision of the Cambridge reference sequence for human mitochondrial DNA, Nat. Genet 23 (2) (1999) 147.

[6] Y.A. Barbitoff, R. Abasov, V.E. Tvorogova, A.S. Glotov, A.V. Predeus, Systematic benchmark of state-of-the-art variant calling pipelines identifies major factors affecting accuracy of coding sequence variant discovery, BMC Genom. 23 (1) (2022) 155.

[7] B. Bekaert, A. Kamalandua, S.C. Zapico, W. Van de Voorde, R. Decorte, Improved age determination of blood and teeth samples using a selected set of DNA methylation markers, Epigenetics 10 (10) (2015) 922–930.

[8] O. Bulbul, G. Filoglu, Development of a SNP panel for predicting biogeographical ancestry and phenotype using massively parallel sequencing, Electrophoresis 39 (21) (2018) 2743–2751.

[9] J.M. Butler, C.R. Hill, M.C. Kline, D.L. Duewer, C.J. Spreche, R.S. McLaren, et al., The single most polymorphic STR Locus: SE33 performance in U.S. populations, Forensic Sci. Int.: Genet. Suppl. Ser. 2 (1) (2009) 23–24.

[10] L. Casanova-Adan, A. Mosquera-Miguel, J. Gonzalez-Bao, A. Ambroa-Conde, J. Ruiz-Ramirez, A. Cabrejas-Olalla, et al., Adapting an established Ampliseq microhaplotype panel to nanopore sequencing through direct PCR, Forensic Sci. Int Genet 67 (2023) 102937.

[11] L. Chaitanya, K. Breslin, S. Zuniga, L. Wirken, E. Pospiech, M. Kukla-Bartoszek, et al., The HIrisPlex-S system for eye, hair and skin colour prediction from DNA: Introduction and forensic developmental validation, Forensic Sci. Int Genet 35 (2018) 123–135.

[12] L. Chaitanya, A. Ralf, van, M. Oven, T. Kupiec, J. Chang, R. Lagace, M. Kayser, Simultaneous Whole Mitochondrial Genome Sequencing with Short Overlapping Amplicons Suitable for Degraded DNA Using the Ion Torrent Personal Genome Machine, Hum. Mutat. 36 (12) (2015) 1236–1247.

[13] Y. Chen, P. Hysi, C. Maj, S. Heilmann-Heimbach, T.D. Spector, F. Liu, M. Kayser, Genetic prediction of male pattern baldness based on large independent datasets, Eur. J. Hum. Genet 31 (3) (2023) 321–328.

[14] G.Y. De La Cerda, J.B. Landis, E. Eifler, A.I. Hernandez, F.W. Li, J. Zhang, et al., Balancing read length and sequencing depth: Optimizing Nanopore long-read sequencing for monocots with an emphasis on the Liliales, Appl. Plant Sci. 11 (3) (2023) e11524.

[15] M. de la Puente, J. Ruiz-Ramirez, A. Ambroa-Conde, C. Xavier, J. Amigo, M. A. Casares de Cal, et al., Broadening the Applicability of a Custom Multi-Platform Panel of Microhaplotypes: Bio-Geographical Ancestry Inference and Expanded Reference Data, Front Genet 11 (2020) 581041.

[16] C. Delahaye, J. Nicolas, Sequencing DNA with nanopores: Troubles and biases, PLoS One 16 (10) (2021) e0257521.

[17] M. Diepenbroek, B. Bayer, K. Schwender, R. Schiller, J. Lim, R. Lagace, K. Anslinger, Evaluation of the Ion AmpliSeq PhenoTrivium Panel: MPS-Based Assay for Ancestry and Phenotype Predictions Challenged by Casework Samples, Genes (Basel) 11 (12) (2020).

[18] M. Fabbri, L. Alfieri, L. Mazdai, P. Frisoni, R.M. Gaudio, M. Neri, Application of Forensic DNA Phenotyping for Prediction of Eye, Hair and Skin Colour in Highly Decomposed Bodies, Healthc. (Basel) 11 (5) (2023).

[19] J. Fleckhaus, P. Bugert, N.A.M. Al-Rashedi, M.A. Rothschild, Investigation of the impact of biogeographic ancestry on DNA methylation based age predictions comparing a Middle East and a Central European population, Forensic Sci. Int Genet 67 (2023) 102923.

[20] K. Fokias, L. Dierckx, W. Van de Voorde, B. Bekaert, Age determination through DNA methylation patterns in fingernails and toenails, Forensic Sci. Int Genet 64 (2023) 102846.

[21] K.J.V. Gaag, S. Desmyter, S. Smit, L. Prieto, T. Sijen, Reducing the Number of Mismatches between Hairs and Buccal References When Analysing mtDNA

[22] Heteroplasmic Variation by Massively Parallel Sequencing, Genes (Basel) 11 (11) (2020).

[23] C. Giuliani, E. Cilli, M.G. Bacalini, C. Pirazzini, M. Sazzini, G. Gruppioni, et al., Inferring chronological age from DNA methylation patterns of human teeth, Am. J. Phys. Anthr. 159 (4) (2016) 585–595.

[23] S.P. Hagenaars, W.D. Hill, S.E. Harris, S.J. Ritchie, G. Davies, D.C. Liewald, et al., Genetic prediction of male pattern baldness, PLoS Genet 13 (2) (2017) e1006594.

[24] C.L. Hall, R.K. Kesharwani, N.R. Phillips, J.V. Planz, F.J. Sedlazeck, R.R. Zascavage, Accurate profiling of forensic autosomal STRs using the Oxford Nanopore Technologies MinION device, Forensic Sci. Int Genet 56 (2022) 102629.

[25] G. Hannum, J. Guinney, L. Zhao, L. Zhang, G. Hughes, S. Sadda, et al., Genome-wide Methylation Profiles Reveal Quantitative Views of Human Aging Rates, Mol. Cell 49 (2) (2013) 359–367.

[26] T. Hao, J. Guo, J. Liu, J. Wang, Z. Liu, X. Cheng, et al., Predicting human age by detecting DNA methylation status in hair, Electrophoresis 42 (11) (2021) 1255–1261.

[27] B.J. Hayes, L.T. Nguyen, M. Forutan, B.N. Engle, H.J. Lamb, J.P. Copley, et al., An Epigenetic Aging Clock for Cattle Using Portable Sequencing Technology, Front. Genet. 12 (2021) 760450.

[28] R.A. Hegele, Molecular forensics: applications, implications and limitations, CMAJ 141 (7) (1989) 668–672.

[29] A. Heidegger, A. Pisarek, M. de la Puente, H. Niederstatter, E. Pospiech, A. Wozniak, et al., Development and inter-laboratory validation of the VISAGE enhanced tool for age estimation from semen using quantitative DNA methylation analysis, Forensic Sci. Int Genet 56 (2022) 102596.

[30] M. Heinrich, M. Muller, S. Rand, B. Brinkmann, C. Hohoff, Allelic drop-out in the STR system ACTBP2 (SE33) as a result of mutations in the primer binding region, Int J. Leg. Med 118 (6) (2004) 361–363.

[31] A.A. Helal, B.T. Saad, M.T. Saad, G.S. Mosaad, K.M. Aboshanab, Evaluation of the Available Variant Calling Tools for Oxford Nanopore Sequencing in Breast Cancer, Genes (Basel) 13 (9) (2022).

[32] S. Hering, J. Edelmann, J. Dressler, Sequence variations in the primer binding regions of the highly polymorphic STR system SE33, Int J. Leg. Med 116 (6) (2002) 365–367.

[33] C. Hollard, C. Keyser, T. Delabarde, A. Gonzalez, C. Vilela Lamego, V. Zvenigorosky, B. Ludes, Case report: on the use of the HID-Ion AmpliSeq Ancestry Panel in a real forensic case, Int J. Leg. Med 131 (2) (2017) 351–358.

[34] J. Hoogenboom, T. Sijen, K.J. van der Gaag, STRNaming: Generating simple, informative names for sequenced STR alleles in a standardised and automated manner, Forensic Sci. Int Genet 52 (2021) 102473.

[35] J. Hoogenboom, K.J. van der Gaag, R.H. de Leeuw, T. Sijen, P. de Knijff, J.F. Laros, FDSTools: A software package for analysis of massively parallel sequencing data with the ability to recognise and correct STR stutter and other PCR or sequencing noise, Forensic Sci. Int Genet 27 (2017) 27–40.

[36] J. Hoogenboom, N. Weiler, L. Busscher, L. Struik, T. Sijen, K.J. van der Gaag, Advancing FDSTools by integrating STRNaming 1.1, Forensic Sci. Int Genet 61 (2022) 102768.

[37] R. Hopman, Opening up forensic DNA phenotyping: the logics of accuracy, commonality and valuing, N. Genet. Soc. 39 (4) (2020) 424–440.

[38] S. Horvath, DNA methylation age of human tissues and cell types, Genome Biol. 14 (R115) (2013).

[39] S. Horvath, M. Gurven, M.E. Levine, B.C. Trumble, H. Kaplan4, H. Allayee, et al., An epigenetic clock analysis of race/ethnicity, sex, and coronary heart disease, Genome Biol. 17 (2016) 171.

[40] C.L.C. Ip, M. Loose, J.R. Tyson, M. de Cesare, B.L. Brown, M. Jain, et al., MinION Analysis and Reference Consortium: Phase 1 data release and analysis, F1000Res 4 (2015) 1075.

[41] A.C. Jager, M.L. Alvarez, C.P. Davis, E. Guzman, Y. Han, L. Way, et al., Developmental validation of the MiSeq FGx Forensic Genomics System for Targeted Next Generation Sequencing in Forensic DNA Casework and Database Laboratories, Forensic Sci. Int Genet 28 (2017) 52–70.

[42] M.J. Jones, S.J. Goodman, M.S. Kobor, DNA methylation and healthy human aging, Aging Cell 14 (2015) 924–932.

[43] M. Kayser, W. Branicki, W. Parson, C. Phillips, Recent advances in Forensic DNA Phenotyping of appearance, ancestry and age, Forensic Sci. Int Genet 65 (2023) 102870.

[44] M. Kolmogorov, K.J. Billingsley, M. Mastoras, M. Meredith, J. Monlong, R. Lorig-Roach, et al., Scalable Nanopore sequencing of human genomes provides a comprehensive view of haplotype-resolved variation and methylation, Nat. Methods 20 (10) (2023) 1483–1492.

[45] B. Koops, M. Schellekens, Forensic DNA Phenotyping: Regulatory Issues, Sci. Technol. Law Rev. 9 (2008).

[46] T. Kubota, K. Lloyd, N. Sakashita, S. Minato, K. Ishida, T. Mitsui, Clog and Release, and Reverse Motions of DNA in a Nanopore, Polym. (Basel) 11 (1) (2019).

[47] H.Y. Lee, S.E. Jung, E.H. Lee, W.I. Yang, K.J. Shin, DNA methylation profiling for a confirmatory test for blood, saliva, semen, vaginal fluid and menstrual blood, Forensic Sci. Int Genet 24 (2016) 75–82.

[48] M.E. Levine, A.T. Lu, A. Quach, B.H. Chen, T.L. Assimes, S. Bandinelli, et al., An epigenetic biomarker of aging for lifespan and healthspan, Aging 10 (4) (2018).

[49] H. Li, Toward better understanding of artifacts in variant calling from high-coverage samples, Bioinformatics 30 (20) (2014) 2843–2851.

[50] H. Li, Minimap2: pairwise alignment for nucleotide sequences, Bioinformatics 34 (18) (2018) 3094–3100.

[51] J. Liu, S. Li, Y. Su, Y. Wen, L. Qin, M. Zhao, et al., A proof-of-principle study: The potential application of MiniHap biomarkers in ancestry inference based on the QNome nanopore sequencing, Forensic Sci. Int Genet 68 (2024) 102947.

[52] G. Liu, Y. Zheng, Q. Wu, T. Feng, Y. Xia, D. Chen, et al., Assessment of ForenSeq mtDNA Whole Genome Kit for forensic application, Int J. Leg. Med 137 (6) (2023) 1693–1703.

[53] A.T. Lu, A. Quach, J.G. Wilson, A.P. Reiner, A. Aviv, K. Raj, et al., DNA methylation GrimAge strongly predicts lifespan and healthspan, Aging 11 (2) (2019).

[54] S. Maestri, M.G. Maturo, E. Cosentino, L. Marcolungo, B. Iadarola, E. Fortunati, et al., A Long-Read Sequencing Approach for Direct Haplotype Phasing in Clinical Settings, Int J. Mol. Sci. 21 (23) (2020).

[55] L.M. McEwen, M.J. Jones, D.T.S. Lin, R.D. Edgar, L.T. Husquin, J.L. MacIsaac, et al., Systematic evaluation of DNA methylation age estimation with common preprocessing methods and the Infinium MethylationEPIC BeadChip array, Clin. Epigenetics 10 (1) (2018) 123.

[56] L.M. McEwen, K.J. O'Donnell, M.G. McGill, R.D. Edgara, M.J. Jones, J.L. MacIsaac, et al., The PedBE clock accurately estimates DNA methylation age in pediatric buccal cells, PNAS 117 (38) (2020) 23329–23335.

[57] A. M'Charek, Silent witness, articulate collective: DNA evidence and the inference of visible traits, Bioethics 22 (9) (2008) 519–528.

[58] P.N. Ossorio, About face: forensic genetic testing for race and visible traits, J. Law Med Ethics 34 (2) (2006) 277–292.

[59] E. Paparazzo, V. Lagani, S. Geracitano, L. Citrigno, M.A. Aceto, A. Malvaso, et al., An ELOVL2-Based Epigenetic Clock for Forensic Age Prediction: A Systematic Review, Int J. Mol. Sci. 24 (3) (2023).

[60] J.L. Park, O.H. Kwon, J.H. Kim, H.S. Yoo, H.C. Lee, K.M. Woo, et al., Identification of body fluid-specific DNA methylation markers for use in forensic science, Forensic Sci. Int Genet 13 (2014) 147–153.

[61] F. Peng, G. Zhu, P.G. Hysi, R.J. Eller, Y. Chen, Y. Li, et al., Genome-Wide Association Studies Identify Multiple Genetic Loci Influencing Eyebrow Color Variation in Europeans, J. Invest Dermatol. 139 (7) (2019) 1601–1605.

[62] V. Pereira, A. Freire-Aradas, D. Ballard, C. Borsting, V. Diez, P. Pruszkowska-Przybylska, et al., Development and validation of the EUROFORGEN NAME (North African and Middle Eastern) ancestry panel, Forensic Sci. Int Genet 42 (2019) 260–267.

[63] R. Pereira, C. Phillips, N. Pinto, C. Santos, S.E. dos Santos, A. Amorim, et al., Straightforward inference of ancestry and admixture proportions through ancestry-informative insertion deletion multiplexing, PLoS One 7 (1) (2012) e29684.

[64] C. Phillips, W. Parson, B. Lundsberg, C. Santos, A. Freire-Aradas, M. Torres, et al., Building a forensic ancestry panel from the ground up: The EUROFORGEN Global AIM-SNP set, Forensic Sci. Int Genet 11 (2014) 13–25.

[65] A. Pisarek, E. Pospiech, A. Heidegger, C. Xavier, A. Papiez, D. Piniewska-Rog, et al., Epigenetic age prediction in semen - marker selection and model development, Aging (Albany NY) 13 (15) (2021) 19145–19164.

[66] plc. ONT. Company history https://nanoporetech.com/about-us/history: Oxford Nanopore Technologies plc.; 2023 [cited 2023 2023-09-08]. Available from: https://nanoporetech.com/about-us/history.

[67] E. Pospiech, Y. Chen, M. Kukla-Bartoszek, K. Breslin, A. Aliferi, J.D. Andersen, et al., Towards broadening Forensic DNA Phenotyping beyond pigmentation: Improving the prediction of head hair shape from DNA, Forensic Sci. Int Genet 37 (2018) 241–251.

[68] E. Pospiech, M. Kukla-Bartoszek, J. Karlowska-Pik, P. Zielinski, A. Wozniak, M. Boron, et al., Exploring the possibility of predicting human head hair greying from DNA using whole-exome and targeted NGS data, BMC Genom. 21 (1) (2020) 538.

[69] A.C. Rand, M. Jain, J.M. Eizenga, A. Musselman-Brown, H.E. Olsen, M. Akeson, B. Paten, Mapping DNA methylation with high-throughput nanopore sequencing, Nat. Methods 14 (4) (2017) 411–413.

[70] Z.L. Ren, J.R. Zhang, X.M. Zhang, X. Liu, Y.F. Lin, H. Bai, et al., Forensic nanopore sequencing of STRs and SNPs using Verogen's ForenSeq DNA Signature Prep Kit and MinION, Int J. Leg. Med 135 (5) (2021) 1685–1693.

[71] Z.L. Ren, J.R. Zhang, X.M. Zhang, X. Liu, Y.F. Lin, H. Bai, et al., Forensic nanopore sequencing of STRs and SNPs using Verogen's ForenSeq DNA Signature Prep Kit and MinION, Int. J. Leg. Med. 135 (2021) 1685–1693.

[72] L. Roewer, M.M. Andersen, J. Ballantyne, J.M. Butler, A. Caliebe, D. Corach, et al., DNA commission of the International Society of Forensic Genetics (ISFG): Recommendations on the interpretation of Y-STR results in forensic analysis, Forensic Sci. Int Genet 48 (2020).

[73] B. Rolf, N. Bulander, P. Wiegand, Insertion-/deletion polymorphisms close to the repeat region of STR loci can cause discordant genotypes with different STR kits, Forensic Sci. Int Genet 5 (4) (2011) 339–341.

[74] J. Ruiz-Ramirez, M. de la Puente, C. Xavier, A. Ambroa-Conde, J. Alvarez-Dios, A. Freire-Aradas, et al., Development and evaluations of the ancestry informative markers of the VISAGE Enhanced Tool for Appearance and Ancestry, Forensic Sci. Int Genet 64 (2023) 102853.

[75] R.R. Salakhov, M.V. Golubenko, N.R. Valiakhmetov, E.N. Pavlyukova, A. A. Zarubin, N.P. Babushkina, et al., Application of Long-Read Nanopore Sequencing to the Search for Mutations in Hypertrophic Cardiomyopathy, Int J. Mol. Sci. 23 (24) (2022).

[76] M. Sasaki, J. Anast, W. Bassett, T. Kawakami, N. Sakuragi, R. Dahiya, Bisulfite conversion-specific and methylation-specific PCR: a sensitive technique for accurate evaluation of CpG methylation, Biochem Biophys. Res Commun. 309 (2) (2003) 305–309.

[77] J.T. Simpson, R.E. Workman, P.C. Zuzarte, M. David, L.J. Dursi, W. Timp, Detecting DNA cytosine methylation using nanopore sequencing, Nat. Methods 14 (2017) 407–410.

[78] Tesi N., Salazar A., Zhang Y., Van der Lee S., Hulsman M., Knoop L., et al. Characterising tandem repeat complexities across long-read sequencing platforms with TREAT. BioRXiv doi: 101101/20240315585288. 2024.

[79] A. Tillmar, K. Sturk-Andreaggi, J. Daniels-Higginbotham, J.T. Thomas, C. Marshall, The FORCE Panel: An All-in-One SNP Marker Set for Confirming Investigative Genetic Genealogy Leads and for General Forensic Applications, Genes (Basel) 12 (12) (2021).

[80] V. Toom, M. Wienroth, A. M'Charek, B. Prainsack, R. Williams, T. Duster, et al., Approaching ethical, legal and social issues of emerging forensic DNA phenotyping (FDP) technologies comprehensively: Reply to 'Forensic DNA phenotyping: Predicting human appearance from crime scene material for investigative purposes' by Manfred Kayser, Forensic Sci. Int Genet 22 (2016) e1–e4.

[81] O. Tytgat, S. Skevin, D. Deforce, F. Van Nieuwerburgh, Nanopore sequencing of a forensic combined STR and SNP multiplex, Forensic Sci. Int Genet 56 (2022) 102621.

[82] I. van Oorschot, A. M'Charek, Keeping race at bay: familial DNA research, the 'Turkish Community,' and the pragmatics of multiple collectives in investigative practice, BioSocieties 16 (2021) 553–573.

[83] S. Walsh, L. Chaitanya, L. Clarisse, L. Wirken, J. Draus-Barini, L. Kovatsi, et al., Developmental validation of the HIrisPlex system: DNA-based eye and hair colour prediction for forensic and anthropological usage, Forensic Sci. Int Genet 9 (2014) 150–161.

[84] S. Walsh, F. Liu, A. Wollstein, L. Kovatsi, A. Ralf, A. Kosiniak-Kamysz, et al., The HIrisPlex system for simultaneous prediction of hair and eye colour from DNA, Forensic Sci. Int.: Genet. 7 (2013) 98–115.

[85] D.Y. Wang, R.L. Green, R.E. Lagace, N.J. Oldroyd, L.K. Hennessy, J.J. Mulero, Identification and secondary structure analysis of a region affecting electrophoretic mobility of the STR locus SE33, Forensic Sci. Int Genet 6 (3) (2012) 310–316.

[86] Y. Wang, Y. Zhao, A. Bollas, Y. Wang, K.F. Au, Nanopore sequencing technology, bioinformatics and applications, Nat. Biotechnol. 39 (2021) 1348–1365.

[87] R.R. Wick, L.M. Judd, K.E. Holt, Performance of neural network basecalling tools for Oxford Nanopore sequencing, Genome Biol. 20 (1) (2019) 129.

[88] A. Wozniak, A. Heidegger, D. Piniewska-Rog, E. Pospiech, C. Xavier, A. Pisarek, et al., Development of the VISAGE enhanced tool and statistical models for epigenetic age estimation in blood, buccal cells and bones, Aging (Albany NY) 13 (5) (2021) 6459–6484.

[89] C. Xavier, M. de la Puente, A. Mosquera-Miguel, A. Freire-Aradas, V. Kalamara, A. Vidaki, et al., Development and validation of the VISAGE AmpliSeq basic tool to predict appearance and ancestry from DNA, Forensic Sci. Int Genet 48 (2020) 102336.

[90] C. Xavier, M. de la Puente, A. Mosquera-Miguel, A. Freire-Aradas, V. Kalamara, A. Ralf, et al., Development and inter-laboratory evaluation of the VISAGE Enhanced Tool for Appearance and Ancestry inference from DNA, Forensic Sci. Int Genet 61 (2022) 102779.

[91] C. Xavier, M. de la Puente, C. Phillips, M. Eduardoff, A. Heidegger, A. Mosquera-Miguel, et al., Forensic evaluation of the Asia Pacific ancestry-informative MAPlex assay, Forensic Sci. Int Genet 48 (2020) 102344.

[92] Z.W. Yuen, S. Shanmuganandam, M. Stanley, S. Jiang, N. Hein, R. Daniel, et al., Profiling age and body fluid DNA methylation markers using nanopore adaptive sampling, Forensic Sci. Int Genet 71 (2024) 103048.

[93] R.R. Zascavage, K. Thorson, J.V. Planz, Nanopore sequencing: An enrichment-free alternative to mitochondrial DNA sequencing, Electrophoresis 40 (2) (2019) 272–280.

[94] Z. Zheng, S. Li, J. Su, A.W. Leung, T.W. Lam, R. Luo, Symphonizing pileup and full-alignment for deep learning-based long-read variant calling, Nat. Comput. Sci. 2 (12) (2022) 797–803.